

Supplement of Hydrol. Earth Syst. Sci., 22, 5143–5158, 2018
<https://doi.org/10.5194/hess-22-5143-2018-supplement>
© Author(s) 2018. This work is distributed under
the Creative Commons Attribution 4.0 License.



Supplement of

Why has catchment evaporation increased in the past 40 years? A data-based study in Austria

Doris Duethmann and Günter Blöschl

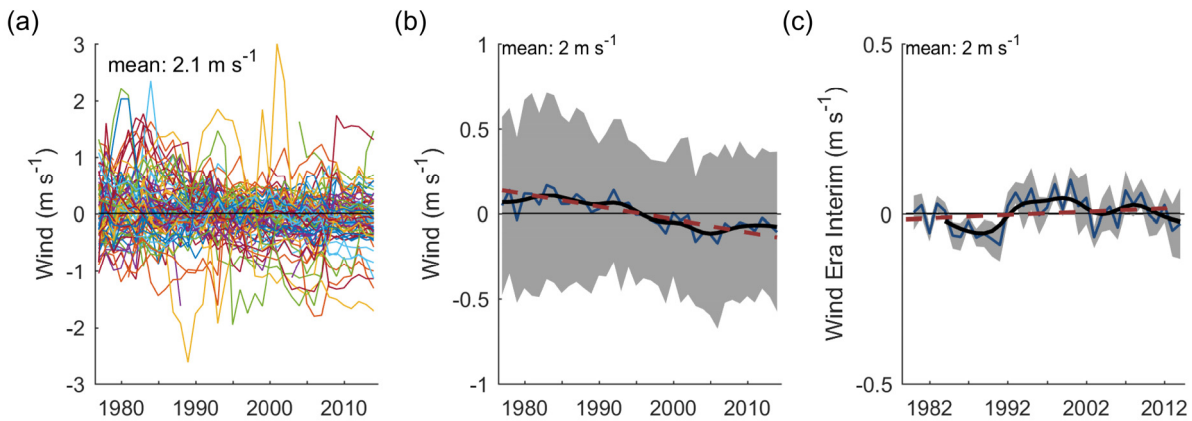
Correspondence to: Doris Duethmann (duethmann@hydro.tuwien.ac.at)

The copyright of individual parts of the supplement might differ from the CC BY 4.0 License.

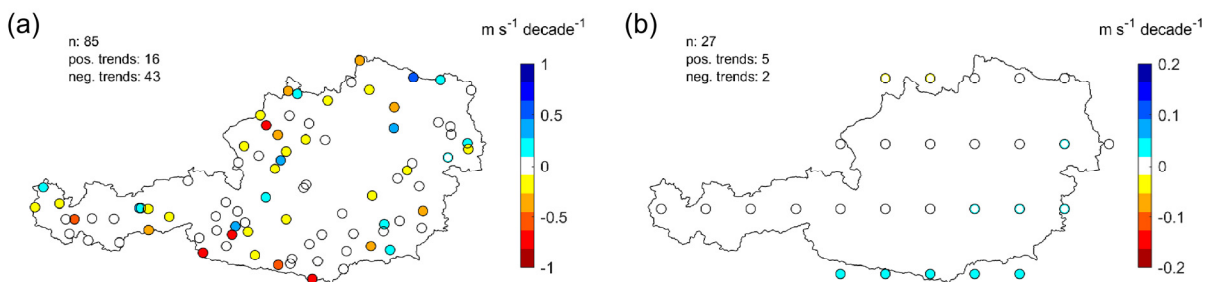
Supplement S1

Wind data

Wind data were regarded as not representative with respect to trends. The reasons for this are: i) annual anomalies of wind speed data from 85 stations in Austria appear unrelated to each other (Supplementary Figure S 1a) and temporal trends over 1977–2014 do not show any spatial pattern (Supplementary Figure S 2a); ii) averaged anomalies of annual wind speeds from station data and ERA Interim data (Dee et al., 2011) show for most part of the series opposing patterns (Supplementary Figure S 2); and iii) wind data are known to be prone to inhomogeneities (Böhm, 2008). We therefore used uniform monthly wind speeds averaged over all years and over all stations in Austria in this study. The potential effect of changes in wind speed was analyzed in Supplement S2.



Supplementary Figure S 1 Anomalies of wind speeds (a, b) from station data (85 stations) over 1977–2014 and (c) from ERA Interim data over Austria (27 grid points) over 1980–2014. (a) Each line refers to one station. (b, c) The thin blue line shows the mean over all catchments, the grey shaded area the variability between catchments (± 1 - standard deviation), the bold black line the smoothed mean (Gaussian filter with a standard deviation of 2 years), and the dashed red line the linear trend.



Supplementary Figure S 2: Spatial pattern of trends in wind speed (a) from 85 stations over 1977–2014 and (b) from ERA Interim data over Austria over 1980–2014. Filled circles indicate significant trends at $p \leq 0.05$.

Analysis of the potential influence of trends in wind speed on reference evaporation

Calculation of E_0 including trends in wind speed

We performed two analyses on the effect of trends in wind speed on E_0 . In the first analysis, we applied average monthly trends derived from station observations of wind speed to the wind speeds used in the original analysis. Heterogeneities in the observations of wind speed (measured at 10 m height) were identified as periods where all annual averages deviate by more than 3 standard deviations from the rest of the series (Vautard et al., 2010) and removed from the series. Series with 3 or more missing years were removed from the data set, which resulted in a data set of 58 stations. We then derived relative trends in monthly wind speeds, averaged these over all stations, and applied them to the wind speeds used in the original analysis.

The second analysis aimed at including spatial heterogeneities in wind speed and its trends. Due to the high spatial heterogeneity of wind speeds, spatial fields of wind speed cannot be directly inferred from the interpolation of the station observations. Spatial fields of average monthly wind speeds were therefore derived as monthly averages from the high-resolution reanalysis data set COSMO-REA6 (Bollmeyer et al., 2015; Kaiser-Weiss et al., 2015), which is based on ERA-Interim (Dee et al., 2011), has a horizontal resolution of about 6 km, and is available during 1995–2015.

Trends in wind speed were again derived from station observations, since downscaled reanalysis data can only capture trends in wind speeds caused by atmospheric circulation changes. Trends caused by changes in surface roughness, caused by changes in land use, for example, cannot be represented (Vautard et al., 2010). The relative trends in monthly wind speeds derived from the station observations were interpolated onto a 1 km grid. In order to focus on the general patterns (i.e. obtain smooth surfaces), a weighted linear least-squares regression (LOWESS method) with a span of 0.75 was used. Gridded fields (1 km resolution) of monthly wind speeds in the period 1977–2014 that represent the general monthly trends were estimated by multiplying absolute values of average monthly wind speeds derived from the reanalysis data with the relative trends derived from the station data:

$$u_{m,t}(x, y) = u_m(x, y) \cdot \left(1 + (t - t_{\text{ave}}) * \frac{\tau_m(x, y)}{100} \right), \quad (S1)$$

where $u_{m,t}(x, y)$ is the wind speed at point (x, y) in month m and year t , $u_m(x, y)$ is the average monthly wind speed (m s^{-1}) at point (x, y) derived from the reanalysis data, $\tau_m(x, y)$ is the trend in monthly wind speed derived from the station data ($\% \text{ y}^{-1}$), t_{ave} is the year represented by the average monthly wind speeds (2004).

For both analyses, E_0 was calculated i) including trends in wind speed, and ii) with average monthly wind speeds of 1994 on a 1 km grid and summarized to catchment averages.

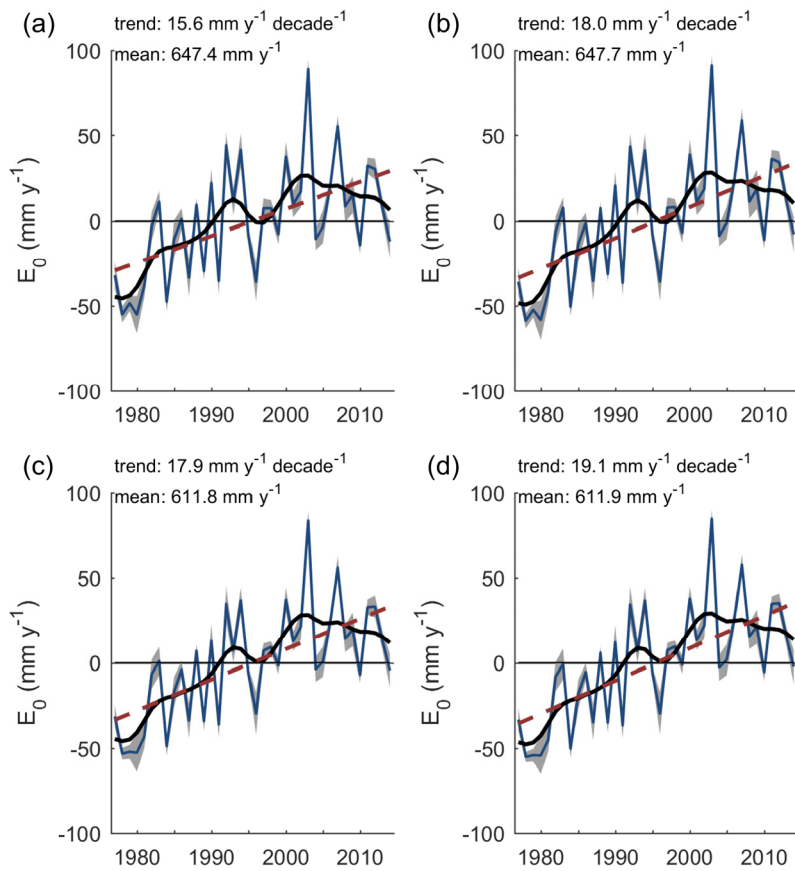
Trends in wind speed and their effect on reference evaporation

The annual trend in wind speed averaged over all stations is $-0.07 \pm 0.06 \text{ m s}^{-1}$ per decade (or $-3.0 \pm 2.5 \%$ per decade) during 1977–2014, which is within the range of the values reported by McVicar et al. (2012) for Europe and very similar to the trend over 276 stations in Europe by Vautard et al. (2010) (-0.09 m s^{-1} per decade or -2.9% per decade during 1979–2008). Trends vary strongly from station to station without a clear spatial pattern. However, the smoothed spatial patterns of trends in wind speed indicate negative wind trends particularly in the southwest of Austria and very small negative or no trends in the east.

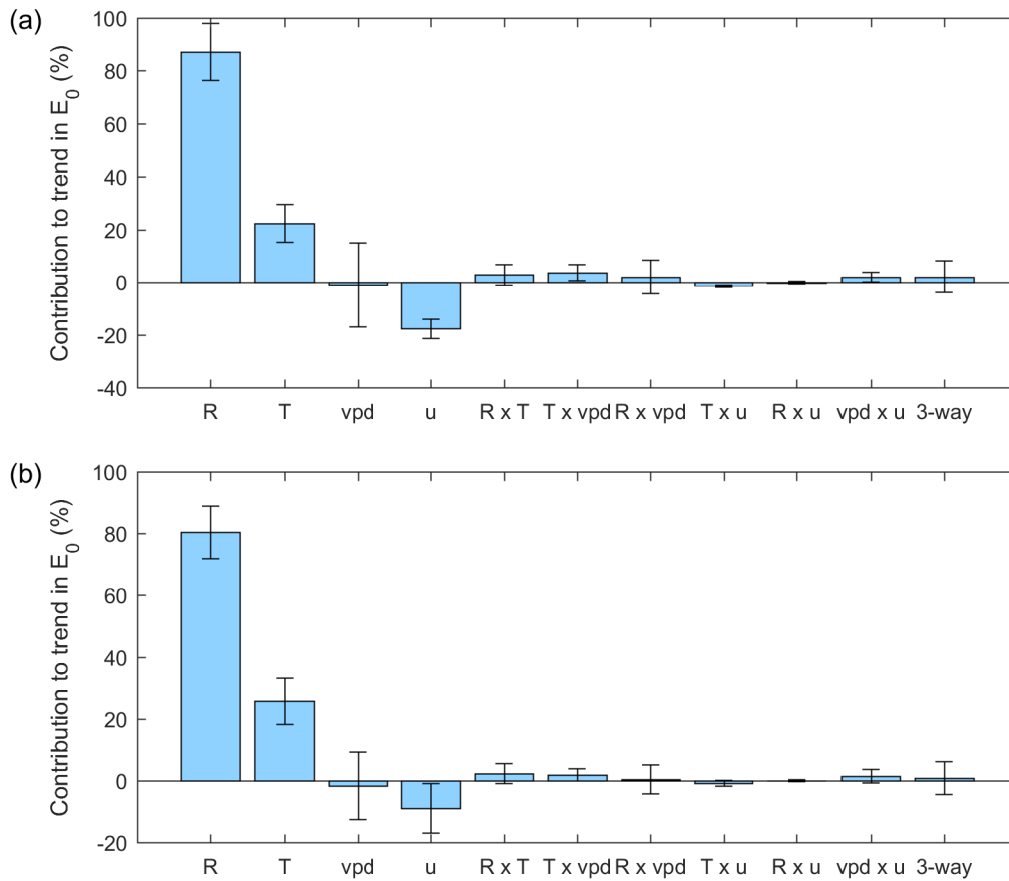
The effect of the trends in wind speed on E_0 is small. According to the first analysis, the trend in E_0 averaged over all catchments is $2.4 \pm 0.7 \%$ per decade when allowing for decreasing wind speeds, as compared to $2.8 \pm 0.7 \%$ per decade when assuming

no trends in wind speed (Supplementary Figure S 3). The direct effects of the changes in net radiation, air temperature and wind speed contributed $87 \pm 11 \%$, $22 \pm 7 \%$, and $-18 \pm 4 \%$ to the trend in E_0 (Supplementary Figure S 4a). In the second analysis, E_0 estimates and trends in wind speed were lower due to lower wind speeds in the reanalysis data compared to the averages of the station data, which led to a smaller effect of the trends in wind speed on E_0 than in the first analysis. When allowing for decreasing wind speeds, the average trend in E_0 is $2.9 \pm 0.6 \%$ per decade, as compared to $3.1 \pm 0.6 \%$ per decade when assuming no trends in wind speed (Supplementary Figure S 3). The direct effects of the changes in net radiation, air temperature and wind speed contributed $80 \pm 9 \%$, $26 \pm 7 \%$, and $-9 \pm 8 \%$ to the trend in E_0 (Supplementary Figure S 4b).

The low influence of the changes in wind speed on E_0 can be explained by the generally humid climate in Austria, where wind speed has a much lower impact on E_0 than in an arid climate (Irmak et al., 2006). The estimated effect of decreasing wind speed may be even lower when the Penman-Monteith equation is coupled to an atmospheric model (van Heerwaarden et al., 2010).



Supplementary Figure S 3 Anomalies of E_0 (a, c) considering trends in wind speed and (b, d) with wind speeds as of 1994 for all years. (a, b) refers to an analysis that applied average monthly relative trends to the wind speeds used in the original study. (c, d) refers to a second analysis that considered spatial heterogeneities in wind speed and its trends. The thin blue line shows the mean over all catchments, the grey shaded area shows the variability between catchments (± 1 SD), the bold black line shows the filtered mean (Gaussian filter with a standard deviation of 2 years), and the dashed red line the linear trend.



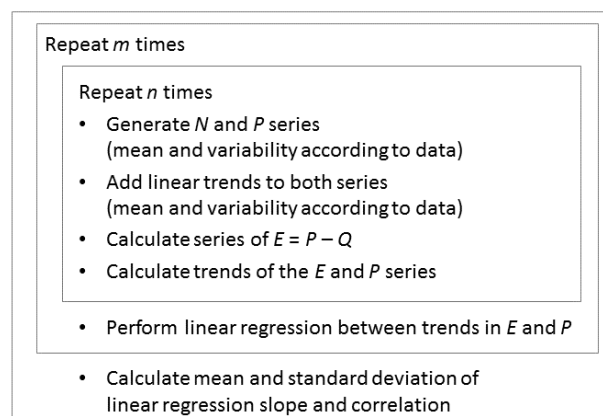
Supplementary Figure S 4 Mean contributions of variations in net radiation (R), air temperature (T), vapor pressure deficit (vpd), wind speed (u), their two-way interaction effects and all three way interaction effects (3-way) to the trend in E_0 . Bars show means over all catchments, error bars show the standard deviation of the variation between catchments. Percent are relative to trends in E_0 . (a) refers to an analysis that applied average monthly relative trends to the wind speeds used in the original study, (b) refers to a second analysis that considered spatial heterogeneities in wind speed and its trends.

5

Monte Carlo simulations for estimating the overestimation of the regression relationship between trends in precipitation and trends in evaporation

Since E_{wb} is estimated from precipitation (P) and discharge (Q), trends in E_{wb} are not independent from trends in P and a regression relationship between these two variables may overestimate the effect of trends in P on trends in E_{wb} . We therefore performed Monte Carlo simulations that aimed at investigating the strength of the relationship between trends in P and trends in E_{wb} resulting from the dependency of the two variables when assuming that trends in E are actually independent of trends in P . The results depend on the assumed statistical properties of the data, amongst others on the spatial variability of the trend in P (the stronger the spatial variability of the P trend, the weaker the relationship when assuming trends in E independent of trends in P). For the Monte Carlo simulations, we generated n correlated, normal distributed series of annual P and annual Q (Supplementary Figure S 5). Means and standard deviations of annual P and Q , and the covariance between annual P and Q were set according to the data set of this study, and n was set to the number of study catchments. Trends in P were considered by adding linear trends to the P series. The variability of the trends between catchments was assumed normal distributed and the mean and variability were derived from the study data. In accordance with the assumption that trends in E are independent of trends in Q , the trend added to the P series was also added to the associated Q series. Annual E series were calculated as P minus Q . Trends in the E and P series were estimated using Sen's slope. We performed a linear regression between trends in E and trends in P over the n data points and calculated the slope and the coefficient of determination. This procedure was repeated $m=1000$ times and the mean and standard deviation of the slope and the coefficient of determination over these m repetitions were calculated.

The resulting regression relationships have a slope of 0.08 ± 0.03 (mean \pm standard deviation) and a correlation coefficient of 0.06 ± 0.04 , suggesting that the slope derived from the regression of E_{wb} against P overestimates the sensitivity of changes in E to changes in P by 0.08 ± 0.03 . The sensitivity of the trend in E_{wb} to trends in P was therefore estimated as the slope of the linear regression between trends in E_{wb} and trends in P corrected by this value.



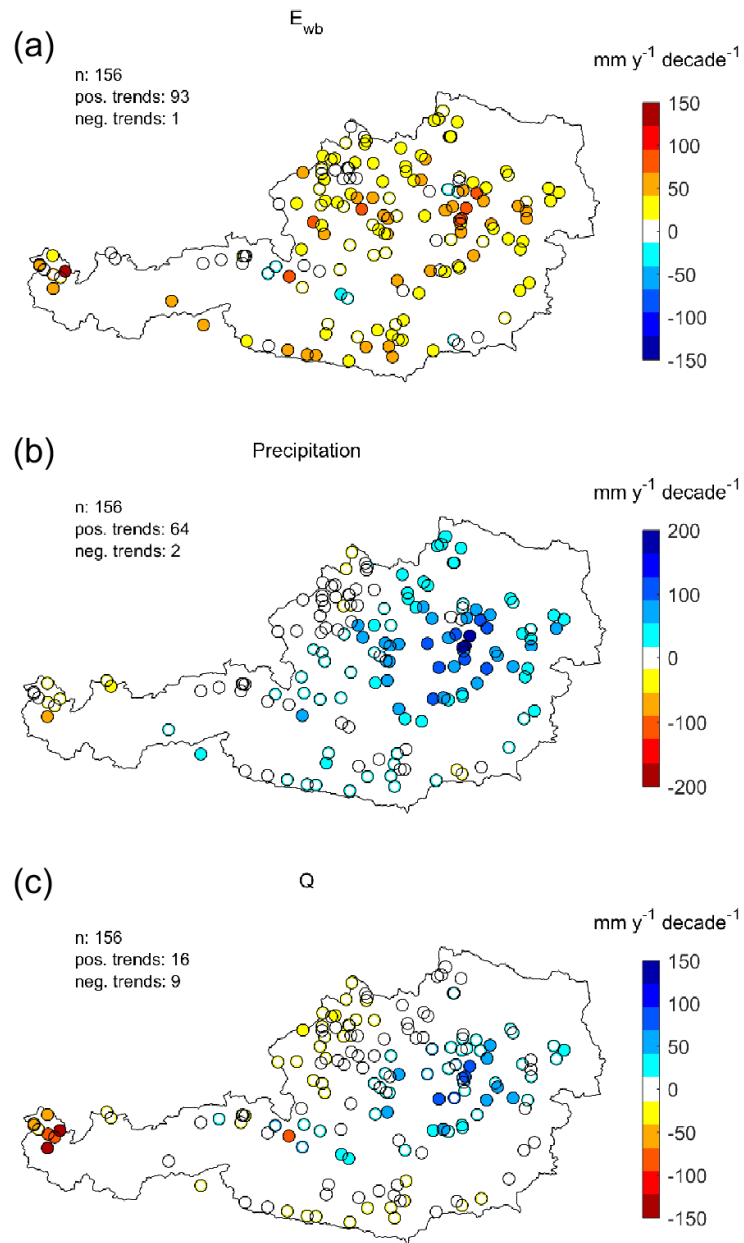
Supplementary Figure S 5 Estimating the overestimation of the regression relationship between trends in precipitation and trends in evaporation, caused by the dependency of the precipitation and evaporation series, by Monte Carlo simulations.

Further supplementary tables and figures

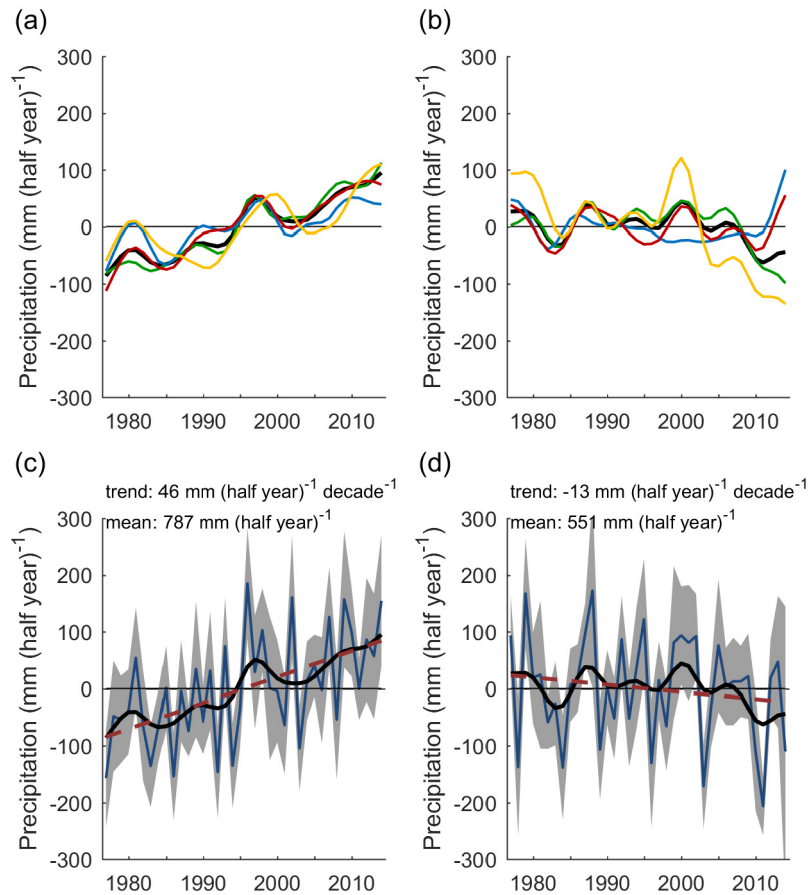
Supplementary Table S 1 Trends in summer (May-Oct) pan evaporation of individual stations in three periods. The table includes the mean, standard deviation (SD), and coefficient of variation (CV) of summer pan evaporation over the available period.

5 Stars indicate trend significance: *** $p \leq 0.01$, ** $p \leq 0.05$, * $p \leq 0.1$

Name	Source	Elev. (m)	East (°)	North (°)	Mean (mm)	SD (mm)	CV (-)	Year start	Year end	Missing data	Trend (% decade ⁻¹)		
											1979-2005	1983-2015	1993-2015
Elmen-Martinau	HZB Tirol	954	10.54	47.36	348	43	0.12	1982	2014	1983	-0.5	-1	3.1
Leutasch-Kirchplatzl	HZB Tirol	1135	11.14	47.37	373	41	0.11	1982	2014	2007	0.6	5.9**	12.2***
Ladis-Neuegg	HZB Tirol	1350	10.65	47.10	400	39	0.10	1982	2014		5.7	2.6	-4.4
St.Johann	HZB Tirol	667	12.44	47.52	336	51	0.15	1982	2014		12.0***	13.1***	13.5***
Aschau	HZB Tirol	1005	12.31	47.38	290	34	0.12	1982	2014		0.2	-2.6	-3.1*
Stetten	HZB Tirol	179	16.38	48.37	369	63	0.17	1992	2014		-	-	9.3
Franzensdorf	HZB Tirol	152	16.64	48.19	382	52	0.14	1992	2014	2010,2011	-	-	-2.9
Hochberg	HZB Tirol	1672	12.36	46.82	373	44	0.12	1983	2014	2008	13.8***	6.2***	3.4
Prägraten	HZB Tirol	1340	12.38	47.02	346	37	0.11	1983	2014		10.8***	4.4*	-1.2
Matrei	HZB Tirol	1040	12.54	47.00	317	48	0.15	1983	2013	2010	-	12.2***	10.1***
Waidring	HZB NÖ	775	12.55	47.59	303	50	0.17	1993	2014	2011	-	-	14.3**
Lunz	HZB NÖ	611	15.07	47.86	292	48	0.17	1992	2014	2010,2013	-	-	-2.1
Frankenfels	HZB NÖ	468	15.33	47.98	293	61	0.21	1993	2014	2007	-	-	22.5***
Ottenstein	HZB NÖ	554	15.34	48.58	336	35	0.10	1994	2014		-	-	5.9
Pyhra	HZB NÖ	298	15.70	48.15	404	44	0.11	1993	2014	2000,2001	-	-	4.4
Hollenthon	HZB NÖ	685	16.26	47.59	369	53	0.14	1993	2014		-	-	6.5
Retz	ZAMG	242	15.95	48.77	424	63	0.15	1975	2005	1987,1995,1996,1997,1998	6.9	-	-
Schwarzenau	ZAMG	500	15.27	48.75	337	38	0.11	1975	2001	1985,1995,1997,1998,1999	-	-	-
Hörsching	ZAMG	298	14.19	48.24	442	60	0.14	1978	2005	1995,1998,2004	5.2	-	-
Wien	ZAMG	163	16.40	48.25	470	73	0.16	1979	2005	1994,1995,1997,1998	12.6***	-	-
Innsbruck Flugh.	ZAMG	579	11.36	47.26	459	64	0.14	1976	2005	1995,1998,2002	6.4	-	-
Vandans	ZAMG	670	9.86	47.09	317	47	0.15	1979	2005	1983,1995,1998,1999,2000	6.8	-	-
Zeltweg	ZAMG	669	14.78	47.20	389	63	0.16	1978	2004	1981,1982,1984,1995,1998	-	-	-
Klagenfurt	ZAMG	447	14.33	46.65	454	81	0.18	1976	2005	1978,1991,1995,1996,1998,2000	13.8**	-	-

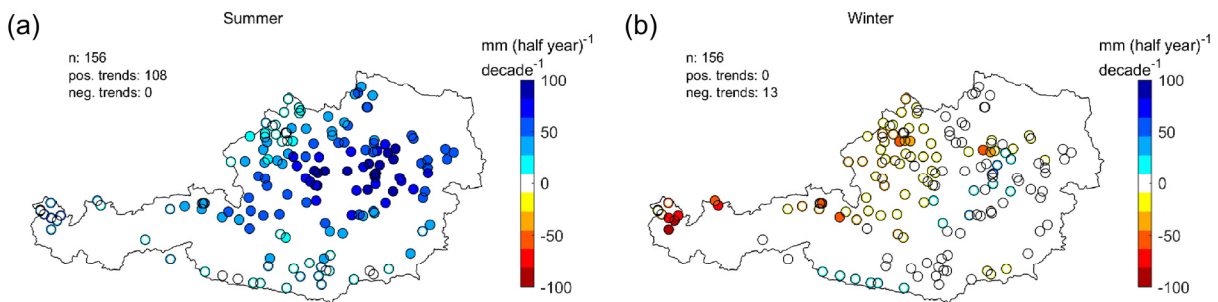


Supplementary Figure S 6 Spatial pattern of trends in (a) E_{wb} , (b) precipitation, and (c) discharge over 1977–2014. Each circle indicates the outlet of one catchment. Filled circles indicate significant trends at $p \leq 0.05$.



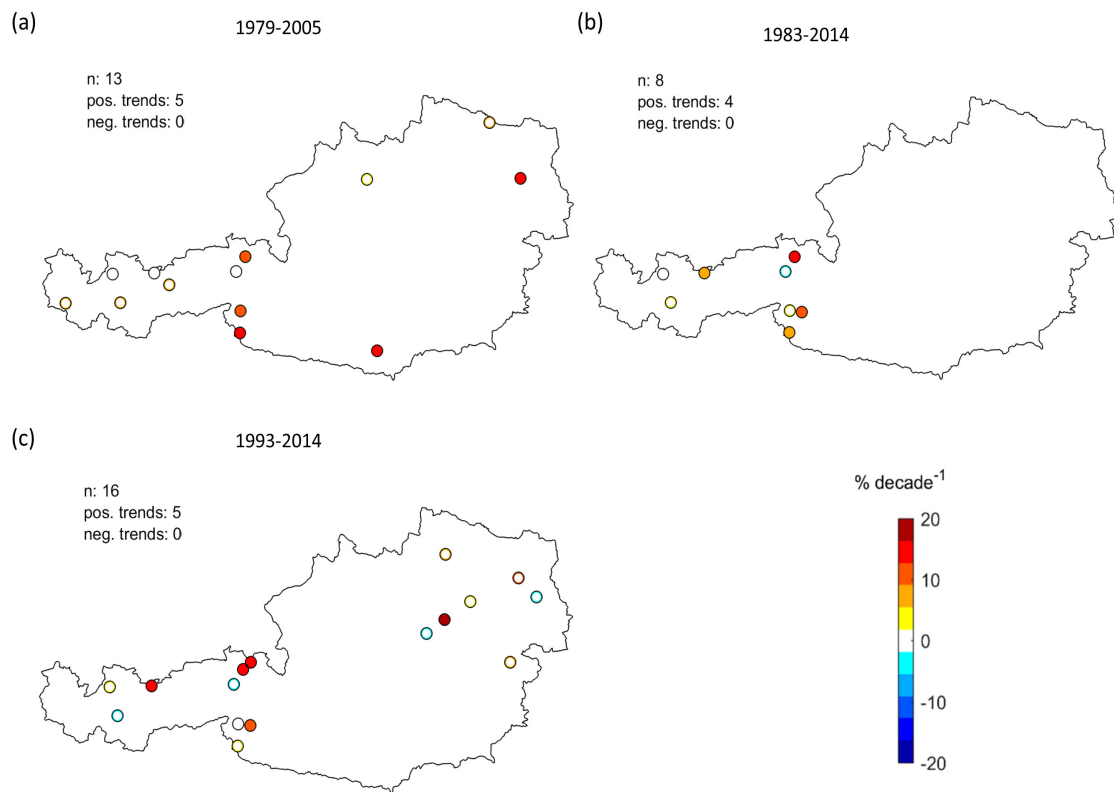
5

Supplementary Figure S 7 Anomalies of (a, c) summer precipitation (May–Oct) and (b, d) winter precipitation (Nov–Apr) over 1977–2014. (a)–(b) mean anomalies by region. Data smoothed using a Gaussian filter with a standard deviation of 2 years. (c)–(d) mean anomalies over all catchments. The thin blue line shows the mean over all catchments, the grey shaded area the variability between catchments (± 1 SD), the bold black line the smoothed mean, and the dashed red line the linear trend.

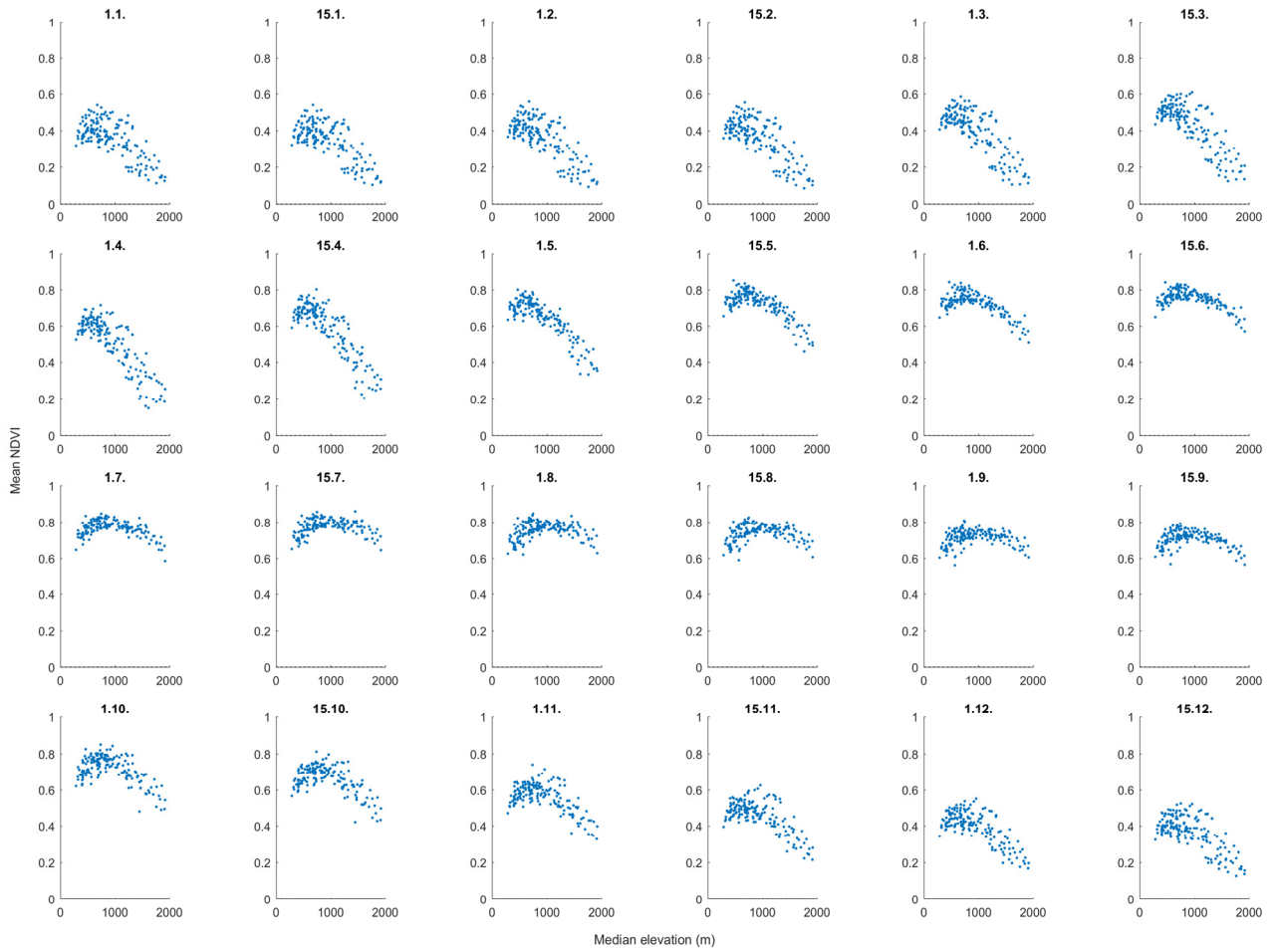


10

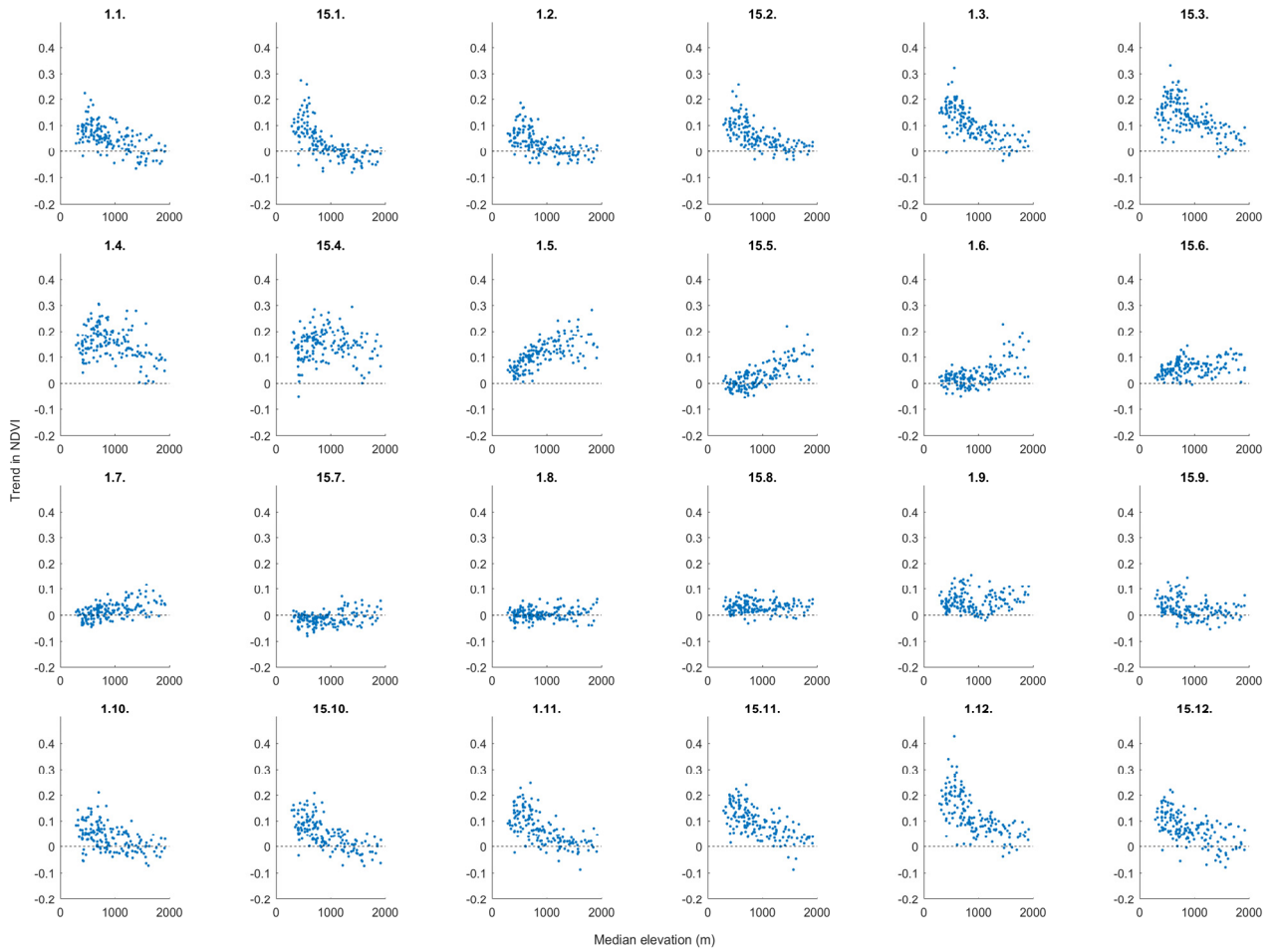
Supplementary Figure S 8 Spatial pattern of trends in (a) summer precipitation (May–Oct) and (b) winter precipitation (Nov–Apr) over 1977–2014. Each circle indicates the outlet of one catchment. Filled circles indicate significant trends at $p \leq 0.05$.



Supplementary Figure S 9 Trends in summer pan evaporation over three different periods. Filled circles indicate significant trends at $p \leq 0.05$.



Supplementary Figure S 10 Scatterplots of the catchment average NDVI (y -axis) versus median catchment elevation (x -axis) for biweekly averages over the course of the year (the plot titles indicate the starting day of the two-week period).



Supplementary Figure S 11 Scatterplots of the catchment average NDVI trend over 1982–2014 (y-axis) versus median catchment elevation (x-axis) for biweekly averages over the course of the year (the plot titles indicate the starting day of the two-week period).

References

- Böhm, R.: Heisse Luft: Reizwort Klimawandel: Fakten, Ängste, Geschäfte, Ed. Va Bene, 2008.
- Bollmeyer, C., Keller, J. D., Ohlwein, C., Wahl, S., Crewell, S., Friederichs, P., Hense, A., Keune, J., Kneifel, S., Pscheidt, I., Redl, S., and Steinke, S.: Towards a high-resolution regional reanalysis for the European CORDEX domain, *Q. J. Roy. Meteor. Soc.*, 141, 1-15, 10.1002/qj.2486, 2015.
- 5 Dee, D. P., Uppala, S. M., Simmons, A. J., Berrisford, P., Poli, P., Kobayashi, S., Andrae, U., Balmaseda, M. A., Balsamo, G., Bauer, P., Bechtold, P., Beljaars, A. C. M., van de Berg, L., Bidlot, J., Bormann, N., Delsol, C., Dragani, R., Fuentes, M., Geer, A. J., Haimberger, L., Healy, S. B., Hersbach, H., Holm, E. V., Isaksen, L., Kallberg, P., Kohler, M., Matricardi, M., McNally, A. P., Monge-Sanz, B. M., Morcrette, J. J., Park, B. K., Peubey, C., de Rosnay, P., Tavolato, C., Thepaut, J. N., and Vitart, F.: The ERA-Interim reanalysis: configuration and performance of the data assimilation system, *Q. J. Roy. Meteor. Soc.*, 137, 553-597, 10.1002/qj.828, 2011.
- 10 Irmak, S., Payero, J. O., Martin, D. L., Irmak, A., and Howell, T. A.: Sensitivity analyses and sensitivity coefficients of standardized daily ASCE-Penman-Monteith equation, *Journal of Irrigation and Drainage Engineering*, 132, 564-578, 10.1061/(asce)0733-9437(2006)132:6(564), 2006.
- 15 Kaiser-Weiss, A. K., Kaspar, F., Heene, V., Borsche, M., Tan, D. G. H., Poli, P., Obregon, A., and Gregow, H.: Comparison of regional and global reanalysis near-surface winds with station observations over Germany, *Advances in Science and Research*, 12, 187-198, 10.5194/asr-12-187-2015, 2015.
- McVicar, T. R., Roderick, M. L., Donohue, R. J., Li, L. T., Van Niel, T. G., Thomas, A., Grieser, J., Jhajharia, D., Himri, Y., Mahowald, N. M., Mescherskaya, A. V., Kruger, A. C., Rehman, S., and Dinpashoh, Y.: Global review and synthesis of trends in observed terrestrial near-surface wind speeds: Implications for evaporation, *J. Hydrol.*, 416, 182-205, 10.1016/j.jhydrol.2011.10.024, 2012.
- 20 van Heerwaarden, C. C., de Arellano, J. V. G., and Teuling, A. J.: Land-atmosphere coupling explains the link between pan evaporation and actual evapotranspiration trends in a changing climate, *Geophys. Res. Lett.*, 37, 10.1029/2010gl045374, 2010.
- 25 Vautard, R., Cattiaux, J., Yiou, P., Thepaut, J. N., and Ciais, P.: Northern Hemisphere atmospheric stilling partly attributed to an increase in surface roughness, *Nature Geoscience*, 3, 756-761, 10.1038/ngeo979, 2010.